EARTH RESEARCH FROM SPACE, 2025, No. 1, pp. 35–46

USING SATELLITE INFORMATION ABOUT THE EARTH

MAPPING OF HYDROTHERMAL-METASOMATIC ALTERATION FOR PREDICTION GOLD MINERALIZATION BASED ON PROCESSING A DATASET OF THE LANDSAT 8 REMOTE SENSING SPACECRAFT FOR THE TERRITORY OF THE EASTERN SLOPE OF THE POLAR URALS

© 2025 Yu. N. Ivanova[a, b, *]

[a] *Institute of Geology of Ore Deposits, Petrography, Mineralogy and Geochemistry of the Russian Academy of Sciences, Moscow, Russia*

[b] *RUDN University, Moscow, Russia*

**e-mail: jnivanova@yandex.ru*

Received June 24, 2024

Abstract. Based on satellite imagery from Landsat 8, an analysis was made of the territories of the eastern slope of the Polar Urals that are promising for identifying gold mineralization (from north to south): Shchuchinskaya zone (Yunyaginskoye deposit), Toupugol-Khanmeishorsky ore district (Novogodnee-Monto and Petropavlovskoye deposits) and the central part of the Malouralskaya zone (Manyukuyu-Vorchatinsky ore cluster). The study was carried out with the aim of identifying similar features in the distribution of metasomatic changes in order to develop a prediction criterion (material) for the gold ore type of mineralization. It was found that in areas promising for Au mineralization on the eastern slope of the Polar Urals, intrusions of basic composition should be localized, with which gold mineralization is genetically associated and metasomatic halos of a significant area (more than 30 km^2) with increased values of iron (III) oxide indices should be localized. And iron (II) oxide, and to a lesser extent — iron oxides and hydroxides (limonite), as well as hydroxyl-(Al-OH, Mg-OH) and carbonate-containing minerals.

Keywords: *gold mineralization, lineaments, morphostructures, hydrothermal-metasomatic alteration, the Polar Urals, Landsat 8*

DOI: 10.31857/S020596142501046e6

INTRODUCTION

Spectral methods of Earth remote sensing (ERS) in the practice of geological exploration began to be used in the 1970s due to the introduction of multispectral photographs of the Earth's surface. Today such methods are widely used along with traditional methods (geological, geophysical, geochemical, etc.) to predict various types of ore mineralization (di Tommaso, Rubinstein 2007; Zhang et al. 2007; Pour, Hashim, 2011; Amer et al., 2012).

The Arctic has recently attracted a lot of attention from scientific communities around the world, and more and more scientific missions are targeting the region because of the vast and diverse mineral resources (MRs) that are still poorly explored.

Many specific challenges in the Arctic, including the prediction of ore deposits, can also be addressed by space-based technologies, which provide many advantages for research and development projects in the area, enabling large-scale and relatively cost-effective observations and data collection in a region with limited ground-based infrastructure (Bohlmanna and Koller, 2020).

Currently, there are very few papers in specialized journals and books devoted to remote sensing on the topic of predicting ore mineralization and mapping metasomatic changes in the Arctic territory (e.g., Pour and Hashim, 2012; Graham et al., 2017; Ivanova et al., 2022, 2023, etc.).

This paper presents the results of mapping of metasomatic change using multispectral satellite images from the Landsat 8 remote sensing spacecraft (RS) for areas of the eastern Polar Urals, part of the Russian Arctic. This study will help to identify a material prediction criterion for gold mineralization, which can be used as an auxiliary tool for MRs exploration in other areas of the Polar Urals and northern latitudes.

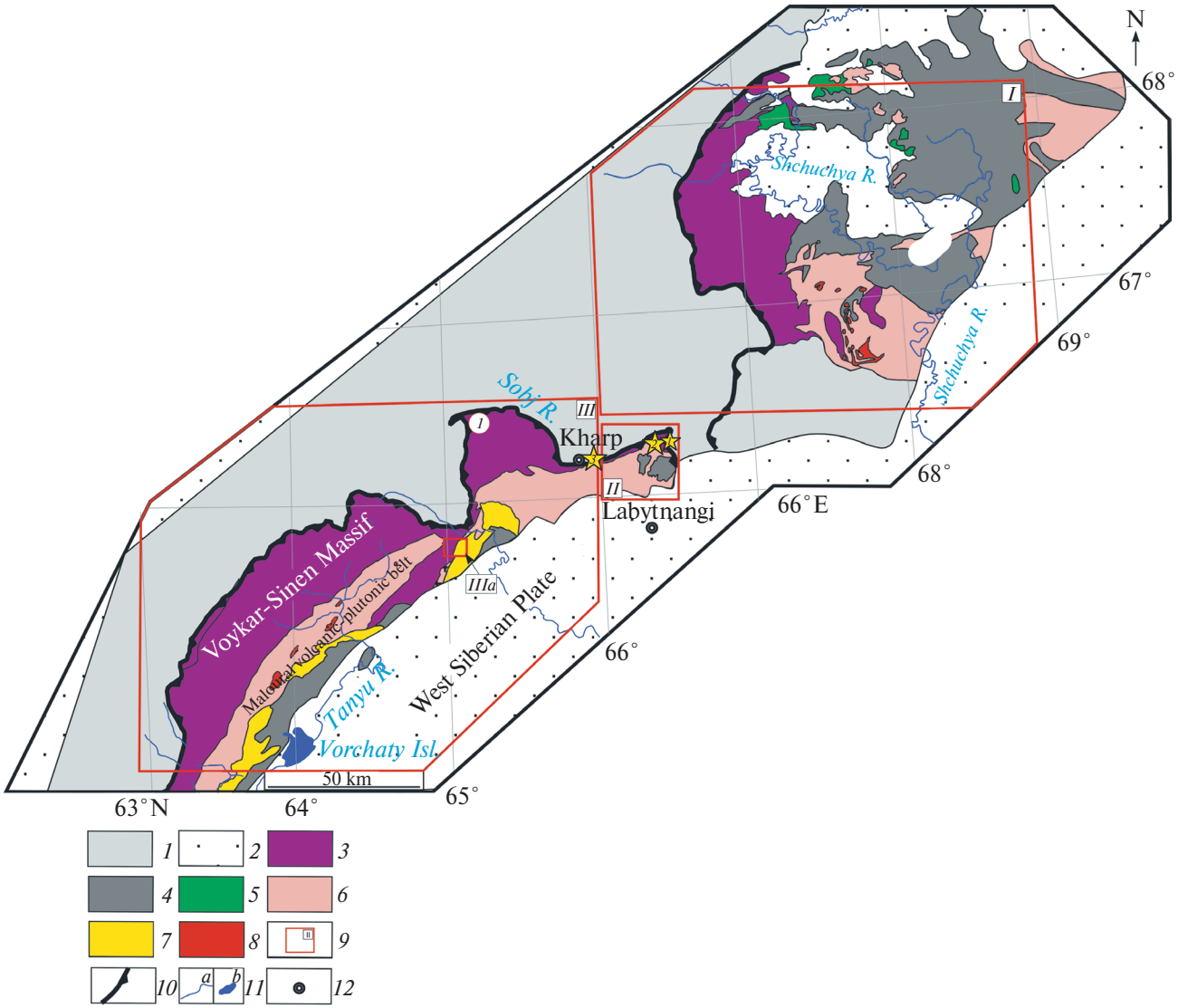

Fig. 1. Tectonic scheme of the Ural fold belt (from State..., 2007): *1* — Late Cambrian and Paleozoic formations of the West Ural structural megazone; *2* — Mesozoic-Cenozoic cover of the West Siberian plate; *3–9* — East Ural megazone (the Shchuchya zone is localized above 66°30'E, the Voykarskaya zone — below 66°30' E): *3* — Ordovician metamorphosed hyperbasites and gabbroids; *4* — Ordovician-Devonian volcanic and volcanogenic-sedimentary formations; *5* — Middle-Late Ordovician gabbroids and plagiogranitoids of the Khoipei complex; *6* — Early-Middle Devonian diorites and granitoids of the Yunyaginsky and Sobsky complexes; *7* — Early-Middle Devonian gabbroids, diorites and monzonitoids of the Kongor complex; *8* — Middle-Late Devonian granitoids of the Yurmenek and Janoslorsk complexes; *9* — boundaries of the studied areas: Shchuchinskaya zone (*I*), Toupugol-Khanmeyshorsky ore district (*II*), central part of Malouralskaya zone (*III*), Manyukuyu-Vorchatinsky ore junction (*IIIa*); *10* — MUF; *11* — main rivers and lake; *12* — towns. Yellow asterisks show: deposits Novogodneye-Monto (1), Petropavlovskoye (2) and ore occurrence Amphibolitovoye (3), number one shows the Rai-Iz massif.

The following areas (from north to south) were selected: Shchuchinskaya zone (Yunyaginskoye deposit), Toupugol-Khanmeyshorsky ore district (Novogodneye-Monto and Petropavlovskoye deposits) and the central part of Malouralskaya zone (Manyukuyu-Vorchatinskoye ore cluster), which are the most promising for identification of gold mineralization.

GEOLOGICAL STRUCTURE OF THE STUDY AREAS

The Polar-Ural segment of the East Ural megazone divided into the Shchuchinskaya and Voykarskaya zones (Fig. 1).

These zones are characterized by sedimentary-volcanogenic deposits with widely manifested

plutonic and hypabyssal magmatism, relatively weak dynamothermal and intense dislocation metamorphism. The formations correspond to the settings of oceanic rifting of island-arc systems and active continental margin (Puchkov and Ivanov, 2020).

The Shchuchinskaya zone is the northernmost part of the Paleozoic island-arc system of the Urals. In the west, it is bounded by a regional fault that is part of the Main Ural Fault (MUF) system. It is a large thrust fault overlain by Mesozoic sediments to the east. Its fragment frames the Shchuchinsky synclinorium in the form of arc-shaped faults that merge into a single semicircular structure.

In the structure of the Shchuchinskaya zone there are several segments, within which the following are established: Paleozoic cover-fold structures represented by rocks of Ordovician, Silurian, Devonian, Carboniferous, overlain by platform Mesozoic sediments of Jurassic and Triassic. The most widespread development among the plutonic formations is represented by gabbroids, granitoids are much less widespread and are localized in the form of small shtokoshaped massifs up to 10–16 km^2 (Dushin, 2020).

For example, manifestations and deposits of V±Ti-Fe-ore and Cu-Fe-scarne formations are associated with magmatic and volcanogenic-sedimentary rocks of the basic composition of the Vaskieu and Harampei-Maslov complexes, as well as the Yanganapei Formation. Sedimentary rocks of Malapaipudynskaya and Khantey formations host occurrences of Pb-Zn mineralization. The magmatic rocks of the main composition of the second phase of the Harbey-Sob complex are associated with manifestations of Mo, Pb-Zn, Cu-quartz and skarn-magnetite mineralization. The magmatic rocks of acidic composition of the Syadatayakhinskiy and Evyuganskiy complexes include deposits and occurrences of As, Au, Mo and Cu mineralization. Cu and Au mineralization is localized in sedimentary rocks of the Khoidyshorsk and Usinskaya Formations, and polymetallic mineralization is localized in metamorphic and sedimentary rocks of the Orang Formation. Cr occurrences are spatially and genetically associated with magmatic rocks of ultrabasic composition of the Syum-Keu complex and dikes of serpentinites of the Hartmannushor complex. Eclogite-like rocks of the Slyudyanogorsk complex contain occurrences of metamorphogenic Ti (Zyleva et al., 2014).

The second phase of the gabbro-granodiorite-granite Yunyaginsky complex can be separately identified for this zone, which is genetically associated with gold-bearing skarn-magnetite deposits and ore occurrences localized in the ore cluster of the same name. The Yunyaginskoye deposit is currently of industrial interest. In addition to this object, the ore cluster hosts a number of ore occurrences and mineralization points of Cu-Fe-ore skarn with Au, Ti-Fe-ore mafic (Volkovsky type), Ti-Fe-ore ultramafic-mafic (Kachkanar type) and Ti-Fe-ore metamorphogenic formations (Zyleva et al., 2014; Andreichev et al., 2017).

The Yunyaginskoye deposit is located 10 km east of the Obskaya-Bovanenkovo railway line. Other known promising ore occurrences and mineralization points are much less well studied.

A more detailed geological description of the Shchuchinskaya zone can be found in articles and published reports (Zyleva et al., 2014; Remizov et al., 2014; Andreichev et al., 2017; Sobolev et al., 2018; Dushin, 2020; Puchkov and Ivanov, 2020, etc.).

The Voykarskaya zone has a submeridional SSW direction and is a series of allochthons dipping gently to the SE. The zone is significantly tectonized and is broken by thrusts into separate plates. The allochthons consist of volcanogenic and terrigenous-volcanogenic rocks of Paleozoic age of oceanic and supra-subduction origin. The footwall of the allochthons (in the western part of the Voykarskaya zone) is bounded by the MUF. The eastern part of the zone is composed of Early-Middle Paleozoic and Late Precambrian blocks of variously metamorphosed ultramafic and basic rocks of ophiolite association. These blocks compose the Rai-Iz and Voykar-Syninsky mountain massifs in the axial part of the Ural Ridge (see Fig. 1). East of the MUF are the Devonian supra-subduction plutonic, hypabyssal, and associated predominantly volcanic and volcanogenic-sedimentary formations (Upper Devonian – Upper Silurian) of the Eastern Subzone (Malouralskaya zone) (Remizov et al., 2014).

In the Middle Paleozoic (Upper Ordovician – Lower Carboniferous), the Malouralskaya zone was either an island arc (Upper Ordovician – Lower Devonian), which was replaced in the Early Devonian by a marginal continental volcanic-plutonic belt (Yazeva and Bochkarev, 1984), or an island arc formed on a heterogeneous basement (Kuznetsov et al., 2000). In the north and west of the Voykara subzone, the Voykar-Syninsky and Rai-Iz massifs are framed from the south and east by a band of gabbro-amphibolites. In the east there are Ordovician-Devonian island-arc plutonic and sedimentary-volcanic complexes, united into the Malouralskaya subzone. In the east of the Malouralskaya subzone, volcanic strata (Upper Ordovician – Middle Devonian) with thin interbeds of sedimentary rocks broken through by intrusions of different compositions (from gabbro to granitoids) come to the surface (State..., 2007). These volcanic strata are part of the Paleozoic island-arc system of the Polar Urals, which developed most likely as a mature island arc in the Eifelian and up to the Permian collision with the East European continent (Estrada et al., 2012; Vikentyev et al., 2017).

The Toupugol-Khanmeyshorsky ore district is localized at the NE end of the Malouralsky volcanic-plutonic belt and represents a local volcanic-tectonic uplift complicating the volcanic-tectonic depression, and is confined to the intersection of submeridional, NE and NW direction fault zones, which limit it and

control the position of gold deposits and occurrences. The NE-direction faults determine the block structure of the ore district and determine the position of intrusive bodies, dikes and apophyses of the Sobsky pluton. All the formations of the district are broken by dikes and sills of gabbro-dolerites and lamprophyres of the Malokhanmei complex (Lower Carboniferous). Two deposits are localized here: Petropavlovskoye (Au-porphyry) and Novogodneye-Monto (Au-Fe-scarn) (see Fig. 1), as well as a number of ore occurrences — Zapadnoye, Karachentseva, Karyernoye, etc. (Fig. 3). (Fig. 3) — of Fe-Au-skarn, gold-quartz and gold-porphyry types (Vikentyev et al., 2017).

The Manukuyu-Vorchatinsky ore cluster consists of volcanogenic and volcanogenic-sedimentary rocks of the Malouralsky Formation (Upper Silurian-Upper Devonian (second phase of the Kongor complex)) interrupted by intrusive formations of the Sobsky and Kongorsky complexes. The suite is characterized by facies uncontainment and is composed of clastic tuffs and tuffites of pyroxene-plagioclase andesibasalts with flows of basalts and andesibasalts, interlayers of tuffites and tuff sandstones. Bioherms composed of reefogenic limestones are occasionally encountered (Shishkin et al., 2009; Kremenetsky et al., 2012). In general, the petrogeochemical composition and petrographic features of volcanic and tuffogenic rocks of the formation indicate that they occurred as a result of explosive activity of central-type volcanoes in a paleogeodynamic setting of subduction stage (Shishkin et al., 2009). The alternation of volcanogenic and sedimentary rock packs in the section indicates periodic activation of volcanic activity during the accumulation of the formation rocks.

Intrusive complexes include formations of the Sobsky (Lower-Middle Devonian) and Kongor (Upper Devonian – Lower Carboniferous) complexes. The Sobsky complex consists of large intrusions of gabbro, diorite, and tonalite that flank a band of volcanics to the west. Small intrusions and dyke formations occurring among the volcanic fields: gabbro, gabbro-diorites, diorites, and montsodiorites are referred to the Kongor complex (Shishkin et al., 2009).

Various objects with iron ore mineralization have been identified here. The most promising are contact-metasomatic (skarn), hydrothermal-sedimentary, magmatic, Ti-magnetite types (First and Third Ore Hills). There are also few manifestations of Ti and Mo mineralization. In addition, Cu mineralization is widely manifested, which is represented both by copper ore and complex objects where Cu is associated with Pb and Zn, Ag, Au, Mo and other metals (manifestations of Yanaslorskoye, Elkoshorskoye, Mokry Log, Osenneye, etc.)

More detailed geological structure of the central part of the Malouralskaya zone and the Toupugol-Khanmeyshorsky ore district can be found in published reports (Galliulin et al, 2005; Perminov et al., 2009, etc.; Butakov et al., 2012; Kremenetsky, 2012; Zyleva et al., 2014; Remizov et al., 2014, etc.) and papers (Chernyaev et al., 2005; Koenig, Butakov, 2013; Vikentyev et al., 2017).

INITIAL DATA

Cloudless daytime scenes of Landsat-8 satellite were obtained:

Shchuchya zone: LC08_L1TP_165012_20161001_20170320_01_T1 (01.10.2016) and LC08_L1TP_165013_20161001_20170320_01_T1 (01.10.2016.); Toupugol-Khanmeyshorsky ore district: LC08_L1TP_165013_20161001_20170320_01_T1 (01.10.2016); central part of Malouralskaya zone: LC08_L1TP_166013_20160821_20170322_01_T1 (21.08.2016).

The images were obtained from the Earth Observation Satellite Data Acquisition and Delivery Information System (EOSDIS) (https://search.earthdata.nasa.gov).

Geological information for the study areas is presented in the form of geologic maps of preQuaternary formations and MRs maps (map scale 1:1000000, sheets Q-41 and Q-42), which were compiled as part of the state assignment of the Karpinsky Institute in 2007 and 2014 (Shishkin et al., 2007; Zyleva et al., 2014).

RESEARCH METHODS

Lineament analysis. Lineaments are straight or approximately linear landforms that are widespread on the Earth's surface and are closely related to the underground hidden and surface structural elements of the discontinuity framework. The orientation and number of lineaments reflect the fracture patterns of rock masses and can carry valuable information about geologic structures, tectonics, and PI localization (e.g., Ekneligoda and Henkel, 2010; Masoud and Koike, 2011).

Lineament analysis is widely used for structural studies (Thannoun, 2013; Milovsky et al., 2021; Ivanchenko et al., 2022), caldera delineation (Ananyev, 2017; Verdiansyah, 2019), assessment of mineralization prospects (Lesniak et al., 2022; Korotkov, 2023), etc.

The methodology for manual lineament extraction based on space images (SI) is given in (Ivanova et al., 2020).

The results of lineament and morphostructural analysis for the study areas can be found in (Vikentiev et al., 2021; Ivanova and Nafigin, 2023; Ivanova, 2024).

Minerals cannot be identified directly by SI, but fields of metasomatic change rocks with pronounced spectral characteristics of absorption and reflection, which are fixed in the range of the remote sensing

satellite sensor, can be identified. Therefore, the band ratio method (band ratios) is widely used to map metasomatic change minerals and lithologic units (Maurer, 2013; Korotkov, 2023). This method enhances the spectral features of image pixels based on the calculation of the ratio of spectral reflectance of one channel to another (Mather, 1999). Such channels are selected based on the reflectance of the mineral being searched for. In this case, the channel characterizing the highest reflecting or emitting ability of mineral should be located in the numerator, and the lowest one in the denominator. As a result, the sought mineral (or their group) will be expressed by bright pixels in the obtained image.

Several mineralogical indices have been developed to map the development fields of metasomotic change minerals using spectral channels of Landsat-8 satellite (Pour et al., 2018): 4/2 — iron oxide and hydroxide group minerals (hematite, magnetite, goethite, ilmenite), as well as jarosite and their mixture — limonite; 6/4 — mineral associations dominated by iron (II) oxide (magnetite); 6/5 — mineral associations with predominance of iron (III) oxide (hematite); 6/7 — hydroxyl-bearing (Al-OH and Fe,Mg-OH), carbonate (calcite and dolomite) and sulfate (gypsum) minerals. These indices are considered as weight indicators (indicators) of Fe^{3+}, Fe^{2+}, Al/Fe-OH, Mg-Fe-OH and Si-OH groups of minerals of hydrothermal nature and products of their hypergenesis.

The principal component analysis (PCA) is a multivariate statistical method that selects uncorrelated linear combinations (eigenvector loadings) of variables such that each extracted component has the smallest variance. More details of the method can be found in (Jolliffe, 2002; Jensen, 2005; Cheng et al., 2006; Gupta, 2017). The first principal component (PC1) is used to extract structural information from the image as it is characterized by the largest variance in the space of all features (Jolliffe, 2002).

PCA converts a correlated data set into uncorrelated linear data. PCA is widely used for mapping metasomatic change minerals and lithologic units based on remote sensing satellite spectral channel-sensors (Loughlin, 1991). This method is applied to the analysis of previously derived mineralogical indices using a covariance matrix. Such an approach allows us to statistically assess the reliability of the spatial distribution of relevant secondary minerals in the study area.

As input data for PCA traditionally act spectral channels of SI, but for the most effective statistical assessment of the reliability of the spatial distribution of relevant hydrothermal minerals in the study area the results of mineralogical indices estimation with the use of covariance matrix were used.

Systematization and generalization of data was performed in QGIS software environment. All available data were collected and visualized in a single GIS project.

RESULTS

For each area, four types of metasomatic change were identified in the SI analysis, represented predominantly by different mineral groups and separately shown in Figs. 2, 3, 5.

For the territory of the Shchuchya zone, the distributions of iron (II) oxide and iron (III) oxide, especially with high content, generally coincide. At that, the greatest accumulation of medium and high concentrations is localized in the north, west and south of the territory. To a lesser extent, the location of elevated values of hydroxyl-(Al-OH, Mg-OH) and carbonate-bearing minerals, and iron oxides and hydroxides (limonite) coincides (see Fig. 2).

This can be explained by the presence of overlying strata in the form of later sedimentary complexes (e.g., the Yany-Manyinsky, Tolya, Teuntoysha and Laborov Formations), which are represented by a variety of sedimentary rocks (sands, gravels, pebbles, conglomerates, lignite beds, siltstones, sandstones, coal clays, clays) up to 450 m thick.

In addition, iron (II) oxide and iron (III) oxide minerals in the ores of the Yunyaginskoye deposit form complex assemblages (poikilitic, myrmekite-like) with both ore (including hematite and pyrite) and nonore minerals (Zyleva et al., 2014).

Researchers of the Karpinsky Institute (Zyleva et al., 2014) have identified beresitization zone in this area, to which objects of Mo, Au, Au-Fe and Pb-Zn mineralization belong (see Fig. 2).

These zones are poorly reflected in the obtained remote sensing results, which is also due to the large thickness of Quaternary sediments. In places where sediments are reduced in thickness, their coincidence is observed (mountainous areas).

The main factors controlling the location of Mo mineralization on the territory of the Shchuchinskaya zone are magmatic (ore-generating acidic intrusions of pre-Ordovician complexes) and hydrothermal-metasomatic (ore-bearing and ore-bearing greisen, vein stockworks).

Most iron ore objects (Cu-Fe-ore skarn (Au-bearing) formation) belong to two genetic types: magmatic and contact-metasomatic. For both, the main ore-controlling factor is also magmatic. The main intrusives are both ore-generating and ore-bearing. Acidic plutonites (Lower-Middle Devonian) provide skarn formation localized exclusively in sedimentary-volcanogenic Silurian strata, which are intruded by granitoids of the Sobsky and Yunyaginsky complexes.

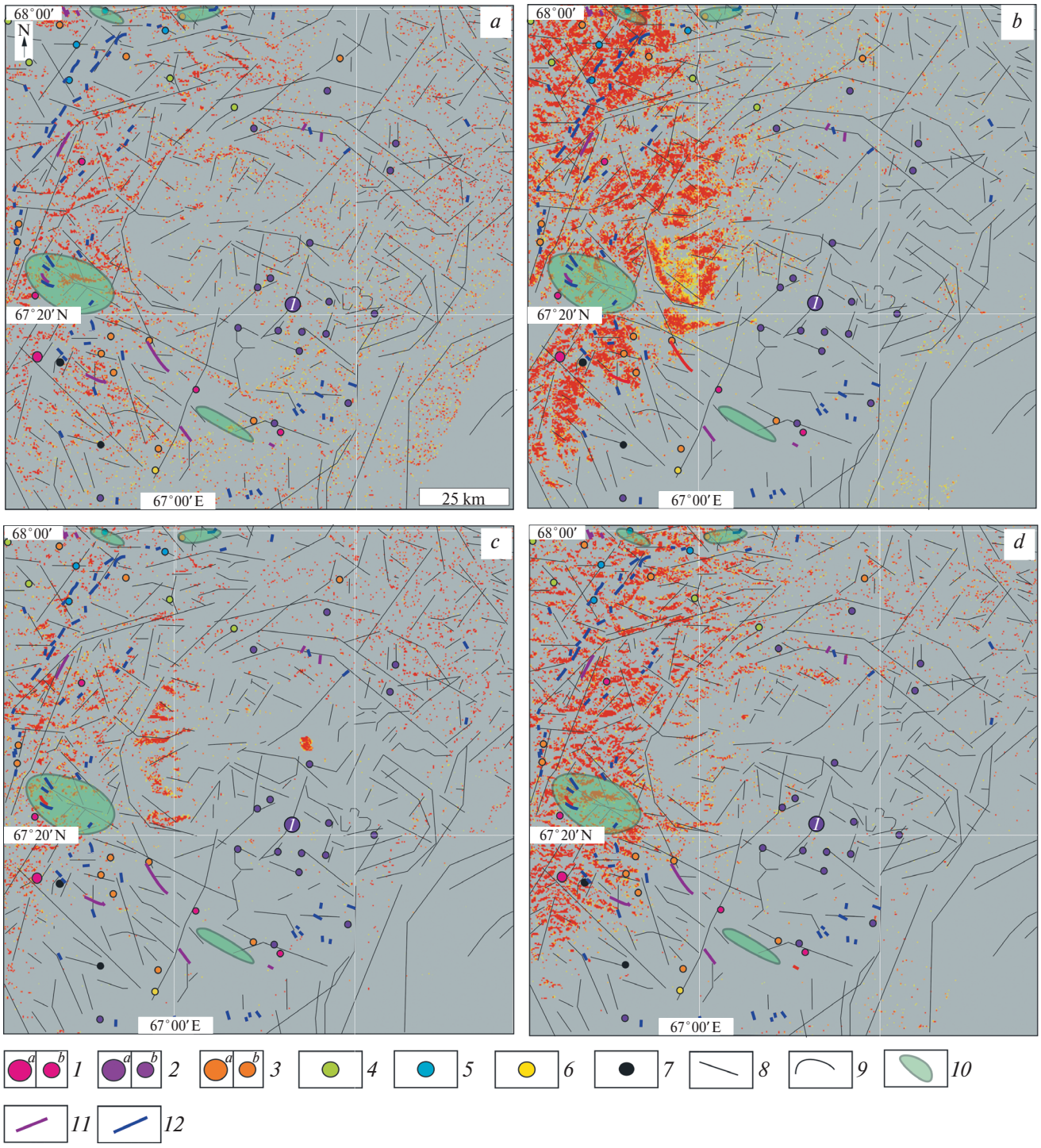

Fig. 2. Schemes of development of metasomatic change mineral associations for the Shchuchinskaya zone, obtained as a result of Landsat 8 satellite SI processing, with lineaments delineated manually, according to Landsat 8 satellite SI: *a* – hydroxyl- (Al-OH, Mg-OH) and carbonate-bearing, *b* — iron (III) oxides (hematite), *c* — iron oxides and hydroxides (limonite), *d* — iron (II) oxides (magnetite). Concentrations of indicator groups of metasomatic changes are shown by colored dots: minimum — yellow, average — orange and maximum — red. *1–7*: deposits (*a*), ore occurrences (*b*): *1* — Mo, *2* — Fe, *3* — Au, Au-Fe, *4* — Cu, *5* — Pb-Zn, *6* — As-Mo-Au, *7* — Ti; *8–9* — radial (*8*) and arc (*9*) lineaments, *10* — beresitization zone, *11–12* — dikes of basic (*11*) and acidic (*12*) composition taken from the geological map (Zyleva et al., 2014). Numder one shows the Yunyaginskoye deposit.

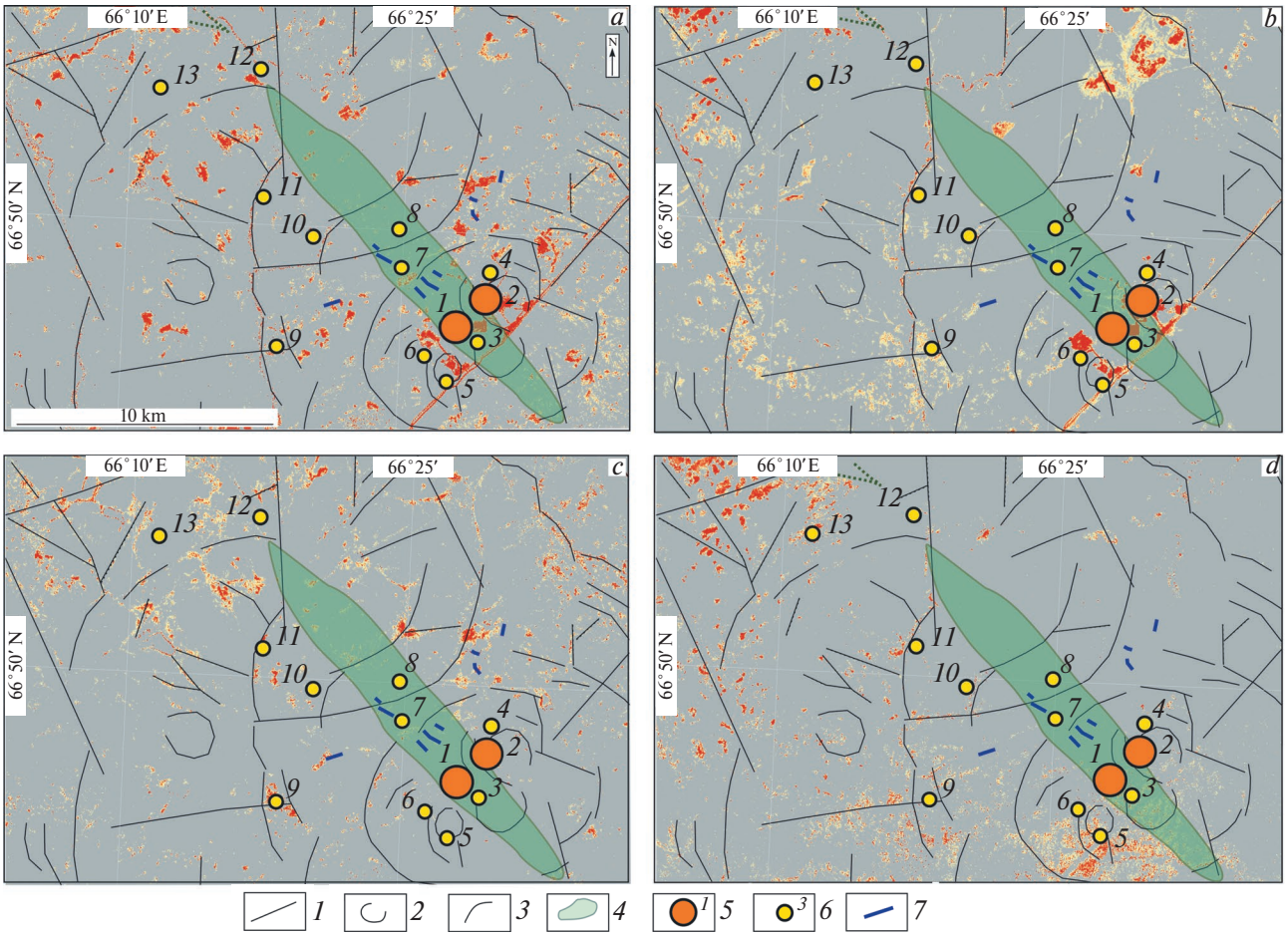

Fig. 3. Map of metasomatic changes of the Toupugol-Khanmeyshorsky ore district and adjacent territory: *a–d* — schemes of development of metasomatic change mineral associations correspond to Fig. 2; *1–3* — lineaments: *1* — radial; *2* — circular; *3* — arc; *4* — beresitization zone taken from the geological map (Zyleva et al, 2014), *5–6* — deposits and ore occurrences: Petropavlovskoye (*1*), Novogodneye-Monto (*2*), Karachentseva (*3*), Toupugol (*4*), Karyernoye (*5*), Taunugolskoye (*6*), Anomalnoye (*7*), Khanmeishorskoye (*8*), Nevidimka (*9*), Obskoye (*10*), Malokhanmeyskoye (*11*), Evyuganskoye (*12*), Evyugan (*13*), *7* — main composition dikes taken from the geological map (Zyleva et al., 2014). Concentrations of indicator groups of metasomatic changes are shown by colored dots: minimum — yellow, average — orange and maximum — red.

In addition, gold mineralization contained in skarn-magnetite deposits and ore occurrences is genetically related to gabbro and diorites.

Pb-Zn mineralization is localized at the contact of gneissed hornblende diorites and apovulcanogenic schists. A “marble-leptite horizon” with a mineral paragenesis close to skarns is distinguished; later beresites develop along the latter (Zyleva et al., 2014).

In the Toupugol-Khanmeyshorsky ore district, the area with the known gold deposits Petropavlovskoye and Novogodneye-Monto is distinguished by the highest concentrations of iron (III) oxide index (see Fig. 3)

The volcanic rocks of medium and basic composition (basalts, andesibasalts, andesites, and less frequently andesites) of the Toupugol Formation are overlain by products of often spatially combined different-age processes of skarnation, beresitization, and silicification. These metasomatic manifestations are associated with dikes of quartz montsodiorite-porphyrites and quartz gabbro of the Congorsk complex of the first and second phases of intrusion (Middle Devonian), as well as propylitization, to which plagiogranites and other granitoids of the late phase of the Sobsky complex were subjected (Middle Devonian). The development of small phenocrysts of Cu and Fe sulfides is associated with propylitization zones, along which sulfide oxidation products develop in the hypergenesis zone (Vikentyev et al., 2021).

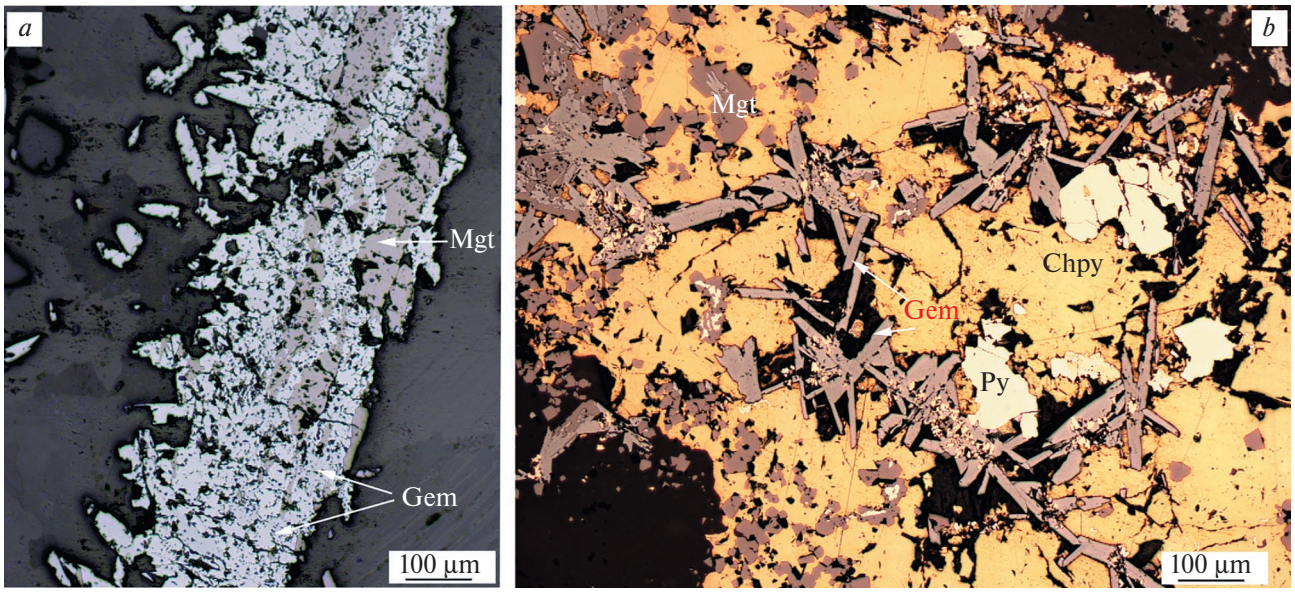

Fig. 4. Decay structures of the Novogodneye-Monto deposit (samples NM-4 and NM-27): allotriomorphic aggregates of hematite replace xenomorphic grains of magnetite in the oxidized skarn (*a*), irregular accumulations of chalcopyrite replace differently oriented needle crystals of hematite and xenomorphic grains of magnetite and pyrite localized in epidote-granate-pyroxene skarn (*b*). Notation: Mgt — magnetite, Py — pyrite, Gem — hematite, Chpy — chalcopyrite.

In addition, iron (II) oxide and iron (III) oxide in the form of concretions and various decay structures can also be found in the Novogodneye-Monto and Petropavlovskoe deposits (Fig. 4).

Researchers of the Karpinsky Institute (Zyleva et al., 2014) identified a beresitization zone with NE-dip in this area, which extends in the NW direction and was traced by boreholes in the Novogodnenskoye ore field to depths of 150–250 m with a gold content of more than 1 ppm. This zone is poorly reflected in the obtained remote sensing results due to the large thickness of Quaternary sediments, which reaches 93 m here (Zyleva et al., 2014). In the SE part of the zone, where the loose sediments, although present, are reduced in thickness to 3–6 m, coincidence is observed. Thus, we can conclude that the halos of near-ore alteration buried for more than 6 m are not reflected on the SI of the day surface.

Deposits and ore occurrences in the central part of the Malouralskaya zone are represented by the following mineralization: Cu-Zn-Mo, Mo-Cu, Fe-Ti-V-Cu and Au.

The most promising objects with iron ore mineralization in this area include contact-metasomatic (skarn), hydrothermal-sedimentary, magmatic, Ti-magnetite types. For example, skarn type occurrences of the First and Third Ore Hills are associated with contact transformation processes.

Manifestations of Ti mineralization are genetically divided into magmatic and sedimentary types. In the former, Ti is associated with iron and is part of titanomagnetite or forms an independent mineral phase — ilmenite. As a rule, rocks of the gabbro family are the most enriched with titanium, where titanium minerals sometimes form scattered phenocrysts and schlierock-like clusters (Sobsky gabbro-diorite-tonalite complex). In addition, the titanomagnetite occurrences have elevated V contents.

Mo mineralization is associated with granitoids and probably belong to the same (stockwork Cu-Mo- or V-Mo-porphyry) geological and industrial type.

Cu mineralization on the area is very widely manifested and is represented both by copper-ore and complex objects, in which Cu is associated with Pb and Zn, Ag, Au, Mo and other metals. For example, mineralization of the Mo-Cu porphyry formation is developed within the Malouralsky volcanic-plutonic belt and is represented by the Yanaslorskoye, Elkoshorskoye, Mokry Log, etc. occurrences. The first of them is localized in granitoids and has predominantly Cu-Mo specialization. The Mokry Log and Osennoe ore occurrences are associated with intrusions of quartz montsodiorites of the Kongorsky complex, which break through volcanogenic-sedimentary rocks of the Malouralskaya Formation. The exocontacts of the intrusions show epidotization, oxidization, and skarnization. The development of quartz-sericite

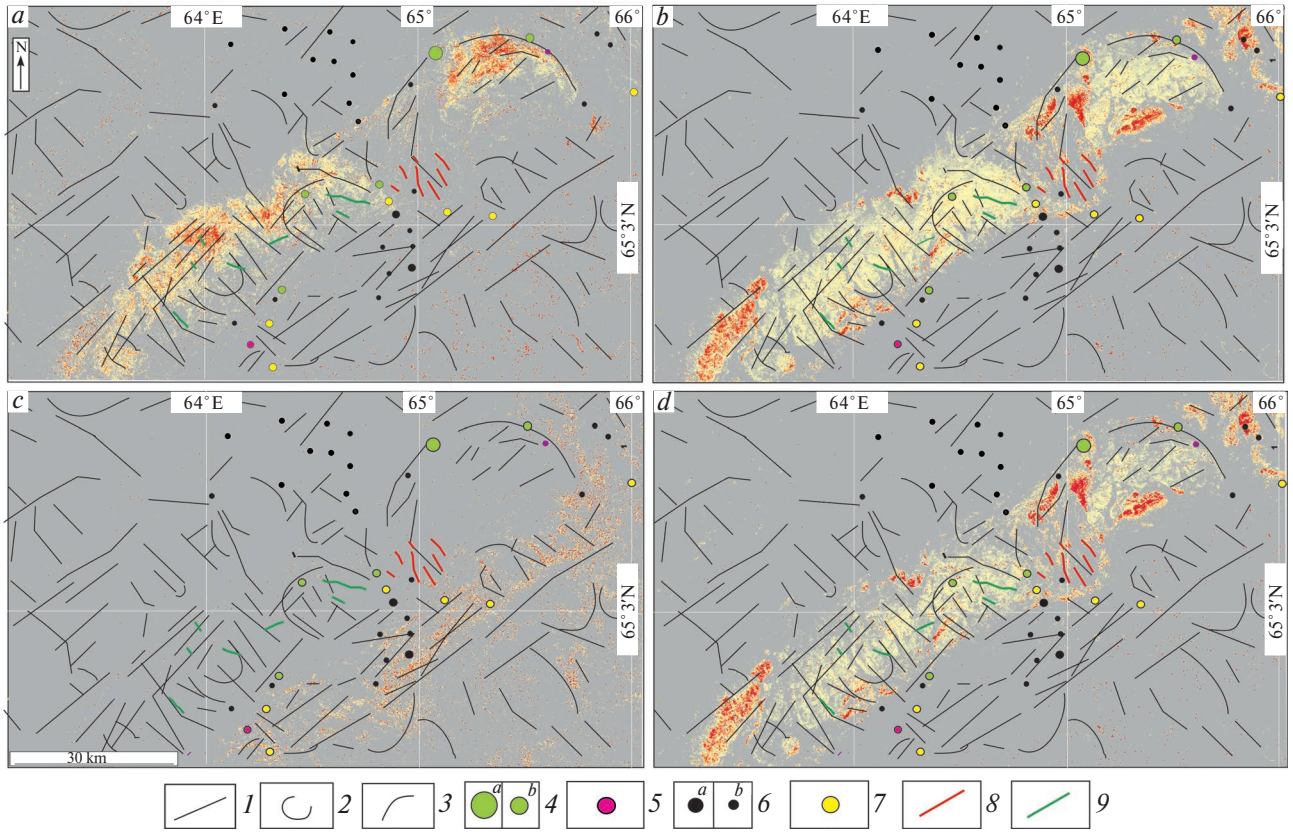

Fig. 5. Map of metasomatic changes of the central part of the Malouralskaya zone and the adjacent territory, obtained with the use of the Landsat 8 remote sensing satellite: *a–d* — correspond to fig. 2: *1–3* — correspond to fig. 3; *4–7* — deposits (*a*) and ore occurrences (*b*): *4* — Cu-Zn-Mo, *5* — Mo-Cu, *6* — Fe-Ti-V-Cu, *7* — Au, *8–9* — dikes of acidic (*8*) and main (*9*) composition taken from the geological map (Shishkin et al., 2009). Concentrations of indicator groups of metasomatic changes are shown by colored dots: minimum — yellow color, average — orange and maximum — red.

metasomatites-phyllisites (berezites) is observed in some areas of the Mokry Log ore occurrence. These formations are accompanied by intense chalcopyrite mineralization (Cu content up to 0.7%).

In addition, the Malouralskaya Formation, consisting of volcanogenic-sedimentary and sedimentary rocks, is a favorable environment for localization of skarn-magnetite and copper porphyry mineralization.

Gold ore objects are paragenetically associated with intrusions and halos of metasomatic change rocks in fault zones (Shishkin et al., 2009).

According to Landsat 8 satellite SI data, the distribution of iron (II) oxide and iron (III) oxide especially with high content, also coincides for the central part of the Malouralskaya zone, but the average concentrations of iron (III) oxide are slightly higher and distributed more evenly over the entire study area than iron (II) oxide (Fig. *5b*, *d*). The distribution of hydroxyl-(Al-OH, Mg-OH) and carbonate-bearing minerals and iron oxides and hydroxides (limonite) are different. The latter are distributed (high and medium concentrations) mainly in the part of the area (see Fig. 5).

The samples of the Amphibolitovoye ore occurrence (central part of the Malouralskaya zone) (see Fig. 1) also contain iron (II) oxide and iron (III) oxide together in the form of various decay structures (Fig. 6) (Ivanova and Tyukova, 2022).

Thus, as a result of the analysis and comparison of areas, the patterns of gold mineralization type for the eastern slope of the Polar Urals have been revealed:

— the studied areas have various ore specialization, including gold ore specialization (Au-sulphide-Fe-skarny), where Au is either the only useful component or one of the main valuable elements (Au containing ore formations: Cu-Fe-skarny, V-Fe-Cu, Cu-Mo-porphyry, etc.). At the same time, gold mineralization has a wide range of formation types: Au-sulfide-quartz veins and vein zones, quartz-Au-sulfide veins, (Cu)-Fe-ore with gold skarn, Cu-porphyry with Au, etc.;

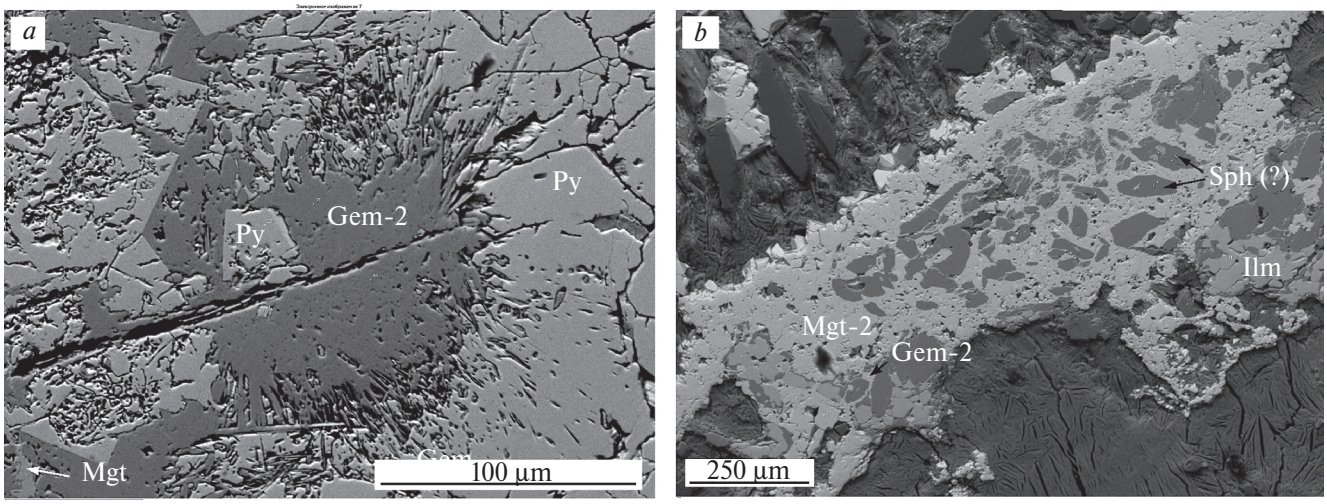

Fig. 6. Decay structures of the Amphibolitovoye ore occurrence (sample A-973): radial aggregate (fibrous structure) of hematite-2, concentrated in cataclastic pyrite localized in pyroxenite (?) (*a*), a loop structure represented by xenomorphic magnetite capturing oval inclusions of sphene (?), xenomorphic inclusions of hematite and ilmenite up to 200 μm are also localized in magnetite, but at the edges of the structure (*b*). Notation: Mgt — magnetite, Py — pyrite, Gem — hematite, Sph — sphene, Ilm — ilmenite.

— According to the conditions of formation, gold mineralization is divided into: (1) magmatic-hydrothermal type — genetically associated with intrusions, which, as a rule, were formed in the epoch close to the formation of the intrusions themselves. (2) Hydrothermal-metamorphogenic type, related to fault zones and confined to halos of metasomatites;

— iron-ore mineralization belongs (Cu-Fe-ore skarn (gold-bearing) formation) mainly to magmatic and contact-metasomatic genetic types (Shchuchinskaya zone and central part of Malouralskaya zone);

— probably, the formation of gold and complex deposits occurred as a result of the development of intracrustal metasomatic systems concentrating ore mineralization. As a result, the decay of such systems in the upper layers of the Earth's crust resulted in the formation of predominantly unextended vertically (not more than 2 km) and small in volume discontinuous columns of ore bodies (Ananyev, 2017);

— the metasomatic halo is manifested over a large area (more than 30 km^2). In areas where, due to the presence of overlying strata, either later sedimentary complexes or a shielding layer of less permeable volcanic rocks, the metasomatic halo is also manifested over a smaller area (up to 10 km^2) (Levochskaya et al., 2021; Gray and Coolbaugh, 1994);

— at microscopic study of ores of samples from deposits and ore occurrences of the studied territories iron (II) oxide and iron (III) oxide are present in the form of various accretions and decay structures.

CONCLUSION

As a result of Landsat 8 remote sensing data processing, maps of metasomatic change distribution were constructed for the territory of the Shchuchinskaya zone, the Toupugol-Khanmeyshorsky ore district and the central part of the Malouralskaya zone: hydroxyl-(Al-OH, Mg-OH) and carbonate-bearing rocks, iron (II) oxide (magnetite) and iron (III) oxide (hematite), iron oxides and hydroxides (limonite), — using spectral channels of Landsat 8 remote sensing satellite (mineralogical indices) and PCA.

Based on the results obtained in the course of the study, it can be concluded that the areas prospective for gold mineralization for the eastern slope of the Polar Urals should be localized intrusions of main composition, with which gold mineralization is genetically related, and metasomatic halos of considerable area (more than 30 km^2) with increased values of iron (III) oxide and iron (II) oxide indices, and to a lesser extent — iron oxides and hydroxides (limonite), as well as hydroxyl-(Al-OH, Mg-OH) and carbonate-bearing minerals.

FUNDING

The work was supported by the youth laboratory of IGEM RAS "Laboratory of prognostic-metallogenic studies" within the framework of the theme of the state assignment "Application of modern methods of assessment, search and forecasting of solid mineral deposits, including

strategic ones, in the Arctic zone of the Russian Federation in order to expand the mineral resource base and plan the development of transportation and communication networks".

REFERENCES

1. *Ananiev Yu.S.* Gold-concentrating systems of the Southern folded framing of the West Siberian plate (on the example of the Western Kalba). Dis. ... dok.geol.-miner. Sciences. Tomsk, 2017, p. 509 (In Russian).

2. *Andreichev V.L., Kulikova K.V., Larionov A.N., Sergeev S.A.* Age of island-arc granites in the Shchuchinskaya zone, Polar Urals: first U–Pb (SIMS) results // Doklady Earth Sciences. 2017. Vol. 477. No. 1. Pp. 1260–1264.

3. *Bohlmanna U.M., Koller V.F.* ESA and the Arctic — The European Space Agency's contributions to a sustainable Arctic // Acta Astronautica. 2020. Vol. 176. Pp. 33–39.

4. *Cheng Q., Jing, L., Panahi A.* Principal component analysis with optimum order sample correlation coefficient for image enhancement // Intern. Jour.of Rem. Sen. 2006. Vol. 27(16). Pp. 3387–3401.

5. *Chernyaev E.V., Chernyaeva E.I., Sedelnikova A.Yu.* Geology of the gold-skarn deposit Novogodnee-Monto (Polar Urals) // Skarns, their genesis and ore content (Fe, Cu, Au, W, Sn, ...). Mat. conf. XI Readings A.N. Zavaritsky. Yekaterinburg: IGiG UrO RAN, 2005. Pp. 131–137.

6. *Di Tommaso I., Rubinstein N.* Hydrothermal alteration mapping using ASTER data in the Infiernillo porphyry deposit, Argentina // Ore Geol. Rev. 2007. Vol. 32. Pp. 275–290.

7. *Dushin V.A.* Geological structure and magmatism of the Shchuchinsky megablock (Polar Urals) // News of the USGU. 2020. Issue. 4(60). Pp. 35–56. (In Russian).

8. *Ekneligoda T.C., Henkel H.* Interactive spatial analysis of lineaments // Jour. of Comp. and Geos. 2010. Vol. 36. No. 8. Pp. 1081–1090.

9. *Estrada S., Henjes-Kunst F., Burgath K.P., Roland N.W., Schäfer F., Khain E.V., Remizov D.N.* Insights into the magmatic and geotectonic history of the Voikar massif, Polar Urals // Zeitschrift der Deutschen Geologischen. Gesellschaft. 2012. Vol. 163. No. 1. Pp. 9–42.

10. *Galiullin I.Z., Perminov I.G., Konovalov Yu.I. et al.* Report on the results of works on completion of the object: "Specialized geochemical prospecting for noble and rare metals in within the West Harbeyskaya area Labytnangi", 2005.

11. *Graham G.E., Kokaly R.F., Kelley K.D. et al.* Application of imaging spectroscopy for mineral exploration in Alaska: a study over porphyry Cu deposits in the Eastern Alaska Range // Econ. Geol. 2018. Vol. 113 (2). Pp. 489–510. DOI: 10.5382/econgeo.2018.4559.

12. *Gray J.E., Coolbaugh M.F.* Geology and geochemistry of Summitville, Colorado: An Epitermal Acid Sulfate Deposit in a Volcanic Dome // Economic Geology. 1994. Vol. 89. Pp. 1906–1923.

13. *Gupta R.P.* Remote Sensing Geology, 3rd edn. Springer, Berlin, Germany, 2017. Pp. 180–190, 235–240, and 332–336.

14. *Ivanchenko G.N., Gorbunova E.M., Cheremnykh A.V.* Some possibilities of lineament analysis when mapping faults of different ranks (using the example of the Baikal region) // Earth Research from Space. 2022. No. 3. Pp. 66–83. (In Russian).

15. *Ivanova J.N., Nafigin I.O.* Application of the Landsat-8 data set and the SRTM digital elevation model to predict gold-base metal mineralization in the central part of the Little Ural zone, Polar Urals // Earth Research from Space. 2023. No. 6. Pp. 20–34. (In Russian).

16. *Ivanova J.N., Tyukova E.E.* Decay structures in the ores of the Amphibolite occurrence (the Polar Urals) // II scientific. conf. "Geology at the Continental Margin". 2022. Pp. 143–145. (In Russian).

17. *Ivanova J.N.* Prediction promising areas for gold ore mineralization based on the integration of geological, geophysical information and processing of the data set of the Earth remote sensing spacecraft Harmonized Landsat Sentinel-2 for the territory of the northern end of the eastern slope of the Polar Urals // Earth Research from Space. 2024 (in press) (In Russian).

18. *Jensen J.R.* Introductory Digital Image Processing: A remote sensing perspective // Pearson Prentice Hall, Upper Saddle River NJ 07458, 3–rd ed., 2005. Pp. 276–287 and 296–301.

19. *Jolliffe I.T.* Principal component analysis. Department of Mathematical Sciences King's College University of Aberdeen, Uk, 2–d edition., 2002. P. 487.

20. *Kenig V.V., Butakov K.V.* Ore gold deposits the Novogodnee-Monto and the Petropavlovskoye are a new gold ore region in the Polar Urals // Razvedka i okhrana nedr. 2013. No. 11. Pp. 22–24. (In Russian).

21. *Korotkov V.V.* Geochemical and other technologies, methods and techniques for forecasting and searching for deposits (mainly "hidden" type) // Federal State Budgetary Institution "VIMS", 2023. P. 166 (In Russian).

22. *Kremenetsky A.A.* Justification of search and prediction and audit works on gold within the Manukuyu-Varchatinsky ore cluster (the Polyarnaya Nadezhda, the Geokhimicheskoe, and the Blagodatnoye ore occurrence). Scale 1: 10,000. Moscow: FSUC IMGRE. 2012. P. 45 (In Russian).

23. *Kuznetsov N.B., Udoratina O.V., Andreichev V.L.* Paleozoic isotope rejuvenation of the pre-Uralide complexes and the problem of the Paleozoic evolution of the eastern margin of the East European continent, Vestn. Voronezh. Gos. Univ., Ser. Geol. 2000. No. 3(9). Pp. 15–19. (In Russian).

24. *Lesnyak D.V., Ananiev Yu.S., Gavrilov R.Yu.* Structural, geophysical and geochemical criteria for epithermal acid-sulfate gold mineralization on the example of the Svetloe ore field (Khabarovsk Territory) // Bulletin of the Tomsk Polytechnic University. Engineering of georesources. 2022. Vol. 333. No. 8. Pp. 60–72. (In Russian).

25. *Levochskaya D.V., Yakich T.Yu., Lesnyak D.V., Ananiev Yu.S.* Hydrothermal-metasomatic zoning, fluid regime and types of gold mineralization in the Emi and Elena sites of the Svetloe epithermal ore field (Khabarovsk Territory) // Proceedings of the Tomsk Polytechnic University. Engineering of georesources. 2021. Vol. 333. No. 10. Pp. 17–34. (In Russian).

26. *Loughlin W.P.* Principal Component Analysis for Alteration Mapping // Photogramm. Eng. Remote Sens. 1991. Vol. 57. Pp. 1163–1169.

27. *Masek J.G., Claverie J., Ju. M. et al.* Harmonized Landsat Sentinel-2 (HLS) Product User Guide. Product Version 2.0. 2018.

28. *Masoud A.A., Koike K.* Morphotectonics inferred from the analysis of topographic lineaments auto-detected from DEMs: application and validation for the Sinai Peninsula, Egypt // Tectonophysics. 2011. 510(3). Pp. 291–308.

29. *Mather P.M.* Computer Processing of Remotely Sensed Images: An Introduction. Chichester, UK: John Wiley and Sons. 1999. P 460.

30. *Maurer T.* How to pan-sharpen images using the gram-Schmidt pan-sharpen method—a recipe. In: International archives of the photogrammetry, remote sensing and spatial information sciences, volume XL-1/W1. ISPRS Hannover workshop, Hannover, pp. 21–2. Environmental Earth Sciences. 2013. 79:101.

31. *Milovsky G.A., Denisova E.A., Yezhov A.A., Kalenkovich N.S.* Asting mineralization in the Sob'-Kharbey area (the Polar Urals) from Geospatial data // The study of the Earth from space. 2007. No. 6. Pp. 29–36. (In Russian).

32. *Perminov I.G., Grigoriev V.V., Kozlitin V.I. al.* Prospecting and prospecting works for ore gold within the Sob-Kharbeyskaya area (YaNAO). Report on works 2006–2009 according to the State Contract No. 111–143 // Labytnangi, the Polar-Ural State Geological Enterprise, 2009. (In Russian).

33. *Pour B.A., Hashim M.* The application of ASTER remote sensing data to porphyry copper and epithermal gold deposits // Ore Geology Review. 2012. Vol. 44. Pp. 1–9. DOI: 10.1016/j.oregeorev.2011.09.009.

34. *Pour A.B., Park Y., Park T.S. et al.* Regional geology mapping using satellite-based remote sensing approach in Northern Victoria Land, Antarctica // Polar Sci. 2018. No. 16. Pp. 23–46.

35. *Pryamonosov A.P., Stepanov A.E., and et al.* State geological map of the Russian Federation. Scale 1:200,000 (second edition). The Polar Ural series. Q-41–XII Sheet. Explanatory note. Salekhard: natural resources committee for the Yamalo-Nenets autonomous district. 2001. P. 231 (In Russian).

36. *Puchkov V.N., Ivanov K.S.* Tectonics of the northern Urals and Western Siberia: general history of development // Geotecto. 2020. No. 1. Pp. 41–61. (In Russian).

37. *Remizov D.N., Shishkin M.A., Grigoriev S.I. et al.* State geological map of the Russian Federation. Scale 1:200,000 (2nd edition, digital). The Polar-Ural series. Sheet Q-41-XVI (Khordyus). Explanatory letter. Saint Petersburg: Cartographic factory VSEGEI. 2014, p. 256 (In Russian).

38. *Shishkin M.A., Astapov A.P., Kabatov N.V. et al.* State geological map of the Russian Federation. Scale 1: 1000000 (3rd gen.). The Ural series. Q41 — Vorkuta sheet: Explanatory note. St. Petersburg: VSEGEI. 2007. P. 541 (In Russian).

39. *Sobolev I.D., Soboleva A.A., Udoratina O.V. et al.* Devonian island-arc magmatism of the Voikar zone in the Polar Urals // Geotectonics. 2018. Vol. 52. No. 5. Pp. 531–563.

40. *Thannoun R.G.* Automatic Extraction and Geospatial Analysis of Lineaments and their Tectonic Significance in some areas of Northern Iraq using Remote Sensing Techniques and GIS // Intern. Jour. of enhanced Res. in Scien. Techn. & Engin. 2013. 2, 2. ISSN NO: 2319–7463.

41. *Verdiansyah O.* A Desktop Study to Determine Mineralization Using Lineament Density Analysis at Kulon Progo Mountains, Yogyakarta and Central Java Province. Indonesia // Indonesian Journ. of Geography. 2019. 51, 1. Pp. 31–41.

42. *Vermote E., Justice C., Claverie M., Franch B.* Preliminary analysis of the performance of the Landsat 8/OLI land surface reflectance product // Remote Sensing of Environment. 2016. Vol. 185. Pp. 46–56.

43. *Vermote E.F., Kotchenova S.* Atmospheric correction for the monitoring of land surfaces // Journal of Geophysical Research: Atmospheres. 2008. Vol. 113(D23).

44. *Vikentiev I.V., Mansurov R.Kh., Ivanova Yu.N. and others.* Gold-porphyry Petropavlovskoe deposit (Polar Urals): geological position, mineralogy and conditions of formation Geology of ores. deposits // Geology of ore deposits. 2017. Vol. 59. No. 6. Pp. 501–541.

45. *Vikentyev I.V., Ivanova Y.N., Tyukova E.E. et al.* Porphyry-style Petropavlovskoe gold deposit, the Polar Urals: geological position, mineralogy, and formation conditions // Geology of Ore Deposits. 2017. Vol. 59. No. 6. Pp. 482–520.

46. *Yazeva R.G., Bochkarev V.V.* Voikar volcano-plutonic belt (Polar Urals). Sverdlovsk: UC AN SSSR, 1984. P. 156 (In Russian).

47. *Zhang X., Panzer M., Duke N.* Lithologic and mineral information extraction for gold exploration using ASTER data in the south Chocolate Mountains (California) // J. Photogram. and Rem. Sens. 2007. Vol. 62. Pp. 271–282.

48. *Zylova L.I., Kazak A.P. et al.* State geological map of the Russian Federation. Scale 1:1000000 (third generation). Series West Siberian. Sheet Q-42 — Salekhard: Explanatory note. Saint Petersburg: VSEGEI, 2014. P. 396 (In Russian).